AAPS PharmSciTech (2020) 21: 33
DOI: 10.1208/s12249-019-1593-7

Research Article

Fibrillated Cellulose *via* High Pressure Homogenization: Analysis and Application for Orodispersible Films

Vincent Lenhart,[1] Julian Quodbach,[1,2] and Peter Kleinebudde[1,3]

Received 30 September 2019; accepted 26 November 2019; published online 20 December 2019

Abstract. Powdered cellulose (PC) and microcrystalline cellulose (MCC) are common excipients in pharmaceuticals. Recent investigations imply that particle size is the most critical parameter for the different performance in many processes. High-pressure homogenization (HPH) was used to reduce fiber size of both grades. The effect of the homogenization parameters on suspension viscosity, particle size, and mechanical properties of casted films was investigated. PC suspensions showed higher apparent viscosities and yield stresses under the same process conditions than MCC. SLS reduced shear viscosity and thixotropic behavior of both cellulose grades probably due to increased electrostatic repulsion. Homogenization reduced cellulose particle sizes, but re-agglomeration was too strong to analyze the particle size correctly. MCC films showed a tensile strength of up to 16.0 MPa and PC films up to 4.1 MPa. PC films disintegrated within 30 s whereas MCC films did not. Mixtures of MCC and PC led to more stable films than PC alone, but these films did not disintegrate anymore. Diclofenac sodium was incorporated in therapeutic dose with drug load of 47% into orodispersible PC films. The content uniformity of these films fulfilled requirements of Ph.Eur and the films disintegrated in 12 s. In summary, PC and MCC showed comparable results after HPH and most differences could be explained by the smaller particle size of MCC suspensions. These results confirm the hypothesis that mainly the fiber size during processing is responsible for the existing differences of MCC and PC in pharmaceutical process, *e.g.*, wet-extrusion/spheronization.

KEY WORDS: microfibrillated cellulose; nanofibrillated cellulose; microcrystalline cellulose; powdered cellulose; orodispersible films.

INTRODUCTION

The sustainable and inexhaustible biopolymer cellulose and its chemically modified derivatives are some of the most used excipients in pharmaceuticals. Due to the possibility of various chemical and physical modifications, cellulose can be used i.a. as dry binder, filling material, viscosity enhancer, and coating polymer (1). Purified cellulose for pharmaceutical purposes is mainly obtained *via* isolation from wood pulp (2). After cellulose isolation, the raw material can be chemically derivatized to create semi-synthetic cellulose for various purposes. Another method to modify the properties of cellulose is the particle size reduction, in particular the fabrication of cellulose fibers in colloidal sizes. A common technique is the high-pressure homogenization of a cellulose slurry for certain cycles at high pressures (3). Depending on the raw material and production technique, the cellulose material is known as microfibrillated cellulose (MFC), nanofibrillated cellulose (NFC), or nanocrystalline cellulose (4).

Beside these modifications, purified cellulose can be milled to obtain powdered cellulose (PC), which is mainly used as filling material in capsules, tablets, and granules. A partial hydrolysis of PC by using mineral acids leads to microcrystalline cellulose (MCC) with a higher crystallinity index and reduced degree of polymerization (DP) (5,6). In many pharmaceutical formulations, MCC has replaced PC because of superior flowability and compactability. In addition, MCC shows unique properties during wet granulation especially during wet extrusion/spheronization processes (7). By adding MCC to a formulation that is intended to form spherical granules, the rheological and mechanical properties are modified to facilitate this process (8). However, PC does not change the wet mass properties in the same manner. Due to

Electronic supplementary material The online version of this article (https://doi.org/10.1208/s12249-019-1593-7) contains supplementary material, which is available to authorized users.

[1] Institute of Pharmaceutics and Biopharmaceutics, Heinrich Heine University Düsseldorf, Universitätsstraße 1, 40225, Dusseldorf, Germany.
[2] Department of Pharmacy, Upsala University, Husargatan 3, 751 23, Uppsala, Sweden.
[3] To whom correspondence should be addressed. (e–mail: kleinebudde@hhu.de)

the fact that PC and MCC are chemically nearly identical, the mechanisms behind the wet extrusion/spheronization process are still not fully understood.

Two hypotheses are established, where the "molecular-sponge" model (9,10) explains the differences with a different water binding behavior during wet massing. MCC particles immobilize water like a sponge and granulation liquid can be squeezed out under shear forces. Other findings, like water migration during extrusion of wet pastes with MCC (11–13) and an increased wet-stage porosity after wet granulation (14), support this hypothesis. However, in all of these studies, PC was not used as negative example and therefore conclusiveness of these findings is limited. Furthermore, Raman spectroscopic investigations do not reveal relevant differences in water binding mechanism of PC and MCC (15). The "crystallite-gel" hypothesis describes MCC as agglomerates of fibers in microscopic and colloidal scale. The colloidal fibers enable, together with the larger cellulose fiber bundles, the formation of a gel like matrix that facilitates wet-extrusion/spheronization processes (16). The existence of these colloidal fibers is the most important distinguishing attribute between PC and MCC. During wet granulation processes, MCC shows a reduction in particle size (17–19) but colloidal particles could not be detected in these studies. Further investigations revealed a dependency of pellet characteristics on the particle size during processing in wet-extrusion/spheronization. Our recent research revealed that even under low shear stress, colloidal particles are liberated by MCC in aqueous medium (20). Therefore, the "crystallite-gel" hypothesis seems to be plausible.

Homogenized cellulose is gaining more attention in pharmaceutical sciences and other fields of research. The homogenized material shows film-forming properties (21) and increased dry binding capabilities (22), probably due to the increased specific surface area/the reduction of particle size and the ability to form coherent matrices more easily (23,24). These findings may also explain the mechanisms during wet-extrusion and spheronization process.

To investigate, if the difference in particle size of PC and MCC is the most important factor for different behavior during wet-granulation processes, PC and MCC were homogenized *via* high-pressure homogenization to reduce particle size. The obtained homogenized cellulose showed interesting properties for pharmaceutical applications and was further investigated as film former in pharmaceutical dosage forms.

MATERIAL AND METHODS

Materials

PC (Arbocel P290, Lot: 7817170702, JRS Pharma GmbH, Germany) and MCC (Vivapur 101, Lot: 6610167248, JRS Pharma GmbH, Germany) were used as starting material for the manufacturing of cellulose suspensions. In some trials, sodium lauryl sulfate (SLS, Caesar & Loretz GmbH, Germany) was used as peptizing agent. Diclofenac sodium (DCS, UNIQUE Chemicals, India) was used as model drug for manufacturing of API loaded films.

Methods

Determination of the Average Molecular Weight and Degree of Polymerization

The average molecular weight/DP of PC and MCC was examined according to monographs of powdered cellulose (Ph.Eur. 01/2017:0315) and microcrystalline cellulose (Ph.Eur. 01/2017:0316). A 1.0 M bis-(ethylenediamine)-copper(II) hydroxide solution (Sigma–Aldrich, USA) was diluted with the same volume of demineralized water and was used as solvent for the samples. The measurements were carried out using a capillary viscosimeter (SI Analytics, Germany) with a capillary diameter of 0.63 mm.

High-Pressure Homogenization

PC was sieved through a 125 μm sieve to remove larger fiber bundles. This procedure should prevent clogging of the homogenization/ball valves of the high-pressure homogenizer (APV 2000, SPX Flow Technology Ltd., United Kingdom). Cellulose was suspended in demineralized water to an absolute cellulose content of 5% (m/m) with a batch size of 500 g for each experiment. Before homogenization, the suspension was mixed using a high shear mixer (Ultra-Turrax TP18/10, IKA–Werke GmbH & Co. KG, Germany) for 1 min at 20,000 rpm. Afterwards, the suspension was homogenized at varying cycles and pressures according to a 2^3 full factorial design. The factors were pressure, number of cycles, and the addition of SLS as peptizing agent (Table 1). The repetitions for the design were carried out at 700 bar, 12 cycles, and 0% of SLS content. For experiments at high pressures and homogenization cycles, a pressure feeding funnel with a maximal feeding pressure of 5 bar was used.

For the manufacturing of the cellulose sheets for pharmaceutical applications, the suspensions were homogenized for 10 cycles at 750 bar. Several PC/MCC mixtures (100%, 90%, 75%, 68.75%, 56.25%, 50%, and 0% (m/m) PC fraction) were used for film manufacturing. The API-loaded films were produced by mixing DCS with pure homogenized PC suspension.

Rheological Properties of MFC Suspension

Viscosity measurements were carried out using a rotary viscometer (Malvern Kinexus, Malvern Instruments Ltd., United Kingdom) equipped with plate–plate (20 mm diameter) geometry at 25°C with a shear-controlled setup. The gap width was set to 500 μm and the shear rates were varied between 0.1 and 100 s^{-1}. The yield stress (τ_y) was estimated by using a fourth order polynomic fit of the shear rate/shear

Table 1. Factor levels of the design of experiments

Factor	−	0	+
Pressure/bar	200	700	1200
Cycles	4	12	20
SLS/%	0	0	0.25

stress graph in a shear rate interval between 0.1 and 1 s^{-1} and calculating the intersection with the *y*-axis. The apparent viscosity (η) was measured at a shear rate of 10 s^{-1}.

Particle Size Distribution

The PSD was measured using laser diffraction (Mastersizer 3000, Malvern Instruments Ltd., United Kingdom) equipped with a wet dispersing unit (Hydro MV, Malvern Instruments Limited, United Kingdom) with demineralized water as dispersing agent. The pump and stirrer speed was set to 2500 rpm. Sonification was not used for dispersing due to uncontrollable artifacts during measurements. For statistical analysis, the median particle size based on volume (x_{50}) was used. The width of the distribution (span) was calculated according to eq. 1. $x_{90/10}$ is the particle size at which 90% or 10% of the particles is smaller.

$$\text{span} = \frac{x_{90} - x_{10}}{x_{50}} \quad (1)$$

Statistical Analysis of Suspension Data

The design and the analysis of the results of the full factorial design were carried out by using MODDE Pro (V12.0.1.3948, Sartorius Stedim Data Analytics AB, Sweden) with multiple linear regression analysis (MLR). If not mentioned elsewhere, the level of significance was $\alpha = 0.05$. If necessary, the responses were transformed logarithmically and marked with a tilde (~).

Manufacturing of the Cellulose Sheets

The homogenized cellulose suspensions were casted out on commercial aluminum foil (Profissimo Aluminiumfolie, dm-drogerie markt GmbH & Co. KG, Germany) *via* solvent casting on an automatic film bench (Coatmaster 500, Erichsen GmbH & Co. KG, Germany). Aluminum foil was used, due to a poor wetting of the available commercial liners. The gap width was set to 1000 μm and casting speed to 120 mm/s. The films of 40 cm length and 22 cm width were dried for 24 h at ambient temperature. After drying, the films were sliced into pieces with the dimensions 2 cm × 3 cm using a disposable scalpel. For determination of the mechanical properties, pieces had the dimensions 2 cm × 12 cm.

Film Characteristics

Mechanical properties were examined using a texture analyzer (TA-XT Plus, Stable Micro Systems Ltd., United Kingdom). Each batch was analyzed at least four times. The measurements were carried out according to ISO 527-1 (25). A specimen with the dimensions 20 × 120 mm was tightened between to clamps. The distance between the clamps was set to 100 mm. The data recording starts at a measured force of 0.01 N. Test speed was set to 10 mm/min. The tensile strength (σ_m), tensile strain at break (ε_B), and Young's modulus (E_t) were calculated according to definitions of the ISO norm. In brief, σ_m was measured at the first maximum in stress in the stress–strain curve. ε_B is the last measured strain value before breakage of the film and E_t is defined as slope of the stress–strain curve between an elongation of 0.05% to 0.25%.

The thickness of 10 films for each batch was measured using a modified micrometer screw (IP65, Mitutoyo Corp., Japan) with two mounting plates with the dimensions 30 * 20 mm at each end. These plates should ensure that the maximum thickness of each film is measured. The weight of films was examined using an analytical balance (CP224S, Sartorius AG, Germany).

To determine the drug loading, 10 API-loaded films with a target dose of 25 mg DCS were individually dispersed in 100 ml 0.1 M NaOH to ensure complete dissolution of the API. The suspension was filtered and 10 ml of each solution was diluted to 100 ml with 0.1 M NaOH. The solution was spectroscopically analyzed with a UV-photometer (UV-1800, Shimadzu Corp., Japan) at a wavelength of 276 nm. Content uniformity and acceptance value was examined according to Ph.Eur. 2.9.40.

The disintegration of the films was tested using a disintegration apparatus (PharmaTest PTZ Auto EZ, PharmaTest Apparatebau AG, Germany) equipped with film holder and a weight of 3 g (PT-ODF) (26). Demineralized water was used as medium and the test was stopped when films did not disintegrate after 3 min.

Scanning Electron Microscopy

The SEM images were taken using an electron microscope (Phenom G2 pro, Phenom World BV, Netherlands). The range of the operating voltage was between 5 and 10 kV. The samples were gold sputtered (Automatic Sputter Coater MSC 1 T, Ingenieurbüro Peter Liebscher, Germany) with a layer thickness of 20 nm.

RESULTS AND DISCUSSION

Effect of Homogenization on Rheological Properties

The settings for the experimental design were selected based on preliminary experiments. Homogenization pressures above 1200 bar led to clogging and excessive heat development during experiments especially in the case of PC. Even sieving of the powder and prior mixing in a high shear mixer did not solve these problems. In addition, the solid content of approximately 5% led to a large viscosity increase and problems with the gravimetric feeding system of the homogenizer. Even the use of a pressurized feeding system did not facilitate a homogenization process with pressures above 1200 bar. The number of homogenization passes was chosen according to literature values used for the production of MFC/ NFC suspensions (27). SLS was incorporated into suspensions to lower fiber–fiber interactions to investigate the effect on particle size and viscosity of the obtained cellulose suspensions. As described in the literature, the homogenization of untreated cellulose mainly leads to MFC. Colloids obtained from partially hydrolyzed cellulose are rather considered as NFC (4).

During homogenization of a cellulose slurry, the suspension showed a continuous viscosity increase. This behavior was attributed to a fibrillation of the cellulose micro- and nanofibrils under high shear stress applied *via* high-pressure

homogenization (28). For both types of cellulose, process conditions had a significant impact on the resulting rheological properties of the cellulose suspensions (Fig. 1). The applied pressure and hence the mechanical energy input in each run did not show a significant effect on the measured τ_y or η. In literature, a positive influence of the pressure on the amount of fibrillated cellulose has been reported (29). The energy needed for the fibrillation of the cellulose slurry may have an optimum and by exceeding this optimum, the agglomeration may dominate due new interfaces growing too fast. Consequently, the new fibers stick together and viscosity does not increase in the expected degree. Analogous to this, a similar behavior has been observed in the homogenization of emulsions and suspensions (30). Nevertheless, the applied pressure determined the minimal size reachable during processing (31) and the pressure showed a positive but non-significant tendency to higher viscosities.

In the selected factor space, the number of homogenization cycles had the largest impact on the measured τ_y and η. During every additional homogenization cycle, more and more fibers were fibrillated and the absolute amount of colloidal fibers increased (32). Similar behavior was already known from emulsions and other colloidal suspension (31,33). Therefore, more homogenization cycles led to a narrower PSD, *i.e.*, more fibers in colloidal sizes and consequently to a higher viscosity of the resulting suspension-like suspension. These observations also fit to the results of Taheri et al. (29) who reported a correlation between number of homogenization cycles and resulting rheological properties. The fitting parameters and transformations of all MLR models can be found in the supplementary materials (Table S1).

The viscosities of PC suspensions, especially at high pressure and high number of cycles, were higher than corresponding MCC suspensions. Homogenization of PC at 700 bar and 12 cycles (P9, P10, and P11, see also Table 2) resulted in an average η of 8.56 ± 2.81 Pa*s. The MCC suspensions manufactured under the same conditions (M9, M10, and M11) showed a η of 2.33 ± 0.57 Pa*s (Table S2). An explanation might be found in the different fiber morphologies of MFC and NFC. The morphology the single fibers might have a high impact on the rheological properties. In this study, single fiber analysis was not possible, but the effect of high-pressure homogenization on obtained colloidal fibers and their aspect ratio is extensively investigated in literature (3,27,34–36). In summary, homogenization of MCC led to fibers with an average diameter of 20 to 100 nm and a length of 100 to 500 nm. In the case of PC, homogenization results in fibers with a similar width, but the length of the fibers can reach several micrometers and therefore result in higher aspect ratios. These longer MFC fibers may result in a suspension with higher viscosity analogous to soluble polymers, where polymers with higher average molecular weight also result in more viscous suspensions for a given solid concentration.

Table 2. Process parameters of produced suspension batches

Batch	Pressure/bar	Number of cycles	SDS content/%
M/P 1	200	4	0
M/P 2	1200	4	0
M/P 3	200	20	0
M/P 4	1200	20	0
M/P 5	200	4	0.25
M/P 6	1200	4	0.25
M/P 7	200	20	0.25
M/P 8	1200	20	0.25
M/P 9	700	12	0
M/P 10	700	12	0
M/P 11	700	12	0

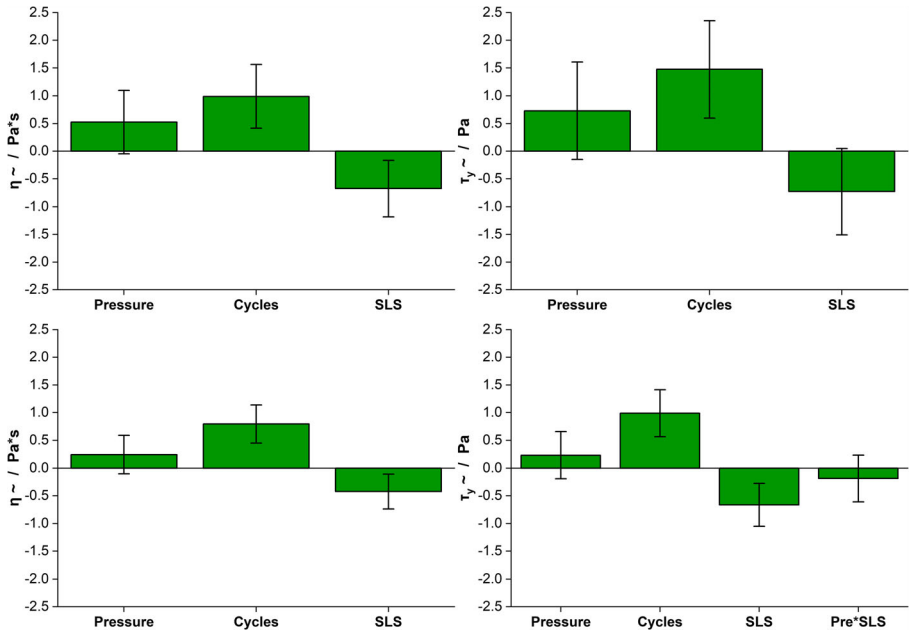

Fig. 1. Coefficient plot of apparent viscosity η apparent yield stress τ_y of PC (upper row) and MCC (lower row)

Effect of SLS on Rheological Properties

The addition of SLS led in all experiments to a lower η and τ_y (Table S3). For instance, the shear viscosity of batch P3 (20 × 200 bar) was reduced by the addition of SLS (batch P7) from 1.4 to 0.2 Pa*s. Similar behavior was observed in case of batch M3 (1.9 Pa*s) and M7 (0.3 Pa*s) (Table S2). Several authors investigated the effect of various surfactants on the rheological properties of cellulose suspensions. It is reported that SLS is able to adsorb on the surface of cellulose preferentially on the more hydrophobic backbone of the polymer (36,37). This adsorption first leads to an increase in viscosity due to micellar bridging phenomena. At higher concentrations, as used in this study (4.76% based on solid content), the electrostatic repulsion might be strongly increased, leading to a reduced fiber–fiber interaction and in consequence to defects in the cellulose matrix and a lower viscosity. For both cellulose grades, SLS reduced the shear viscosity up to one order of magnitude. PC seemed to be more sensitive to the addition of SLS than MCC. MCC, as a partially hydrolyzed form of PC, showed a particle size reduction even under low stress (19) and in part to colloidal sizes (20). For PC, this behavior could not be verified. Consequently, MCC needed less energy to release a larger amount of colloidal fibers and the particles had a higher specific surface area. Accordingly, the surface saturation level and zeta potential should be higher for PC suspensions, leading to an even stronger weakening of the cellulose matrix.

All produced cellulose suspensions showed shear thinning with a hysteresis upon lowering the shear rate after reaching maximum shear rate (Figs. 2 and 3). This behavior is attributed to the formation of a coherent cellulose fiber network after homogenization (37). Under shear stress, the coherent cellulose matrix breaks down, the fibers reorient in the direction of shear and resistance against shearing reduces. By lowering the shear forces again, the network slowly regenerates. The time dependency of the matrix regeneration was not investigated, but other authors reported a full recovery of rheological properties for cellulose suspensions (35). Not all batches showed a measurable τ_y (Table S2). At low pressures and/or low number of cycles, the volumetric fraction of the colloidal fibers was probably too low to form a coherent fiber matrix. But this formation is a substantial criterion for the existence of gel characteristics. Xu et al. (23) and Moberg et al. (24) have reported a dependency of the necessary volume fraction of colloidal fibers and reached viscosity on the fiber dimensions, *i.e.*, the aspect ratio of the fibers. The calculated percolation limit has varied between 0.31 and 1.99% depending on the size and the origin of the used material. In our study, cellulose was used with a weight percentage of approx. 5% (≈ 3.3% by volume) and therefore clearly above the percolation limit. Only after sufficient shear stress and homogenization time, the volumetric fraction of colloids might be high enough to form a coherent matrix together with the larger fibers.

SLS also seemed to affect the thixotropy of the cellulose suspensions. The hysteresis of P7 (20 × 1200 bar with SLS) was much smaller than P3, which indicated stronger thixotropic behavior of P3 (20 × 1200 bar without SLS) (Fig. 2). It can be concluded that homogenization parameters, especially the number of cycles, have an influence on the resulting viscosity. These changes in viscosity should be mainly caused by a reduction of the particle size into colloidal ranges.

Effect of Homogenization on the Particle Sizes

The results of viscosity analysis and particle size examination were not consistent, and no clear correlation could be found. It should be noted that particle sizes can vary between 0.1 and 100 μm, *i.e.*, four orders of magnitude. Laser

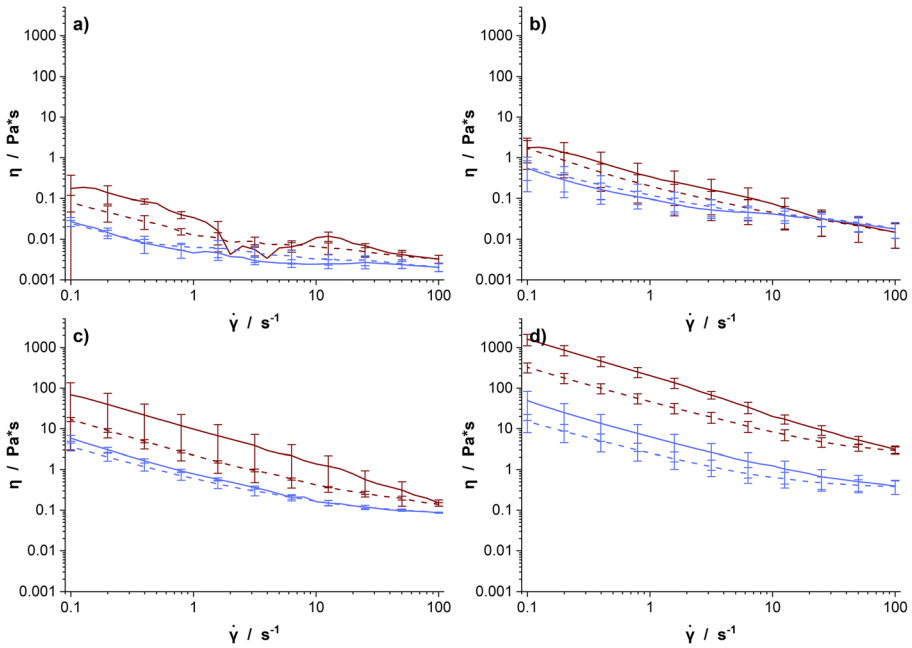

Fig. 2. Rheological investigation of PC suspensions with (−) and without SLS (−) addition. **a** P1 and P5, **b** P2 and P6, **c** P3 and P7, and **d** P4 and P8. Solid lines represent increasing shear rates and dashed lines decreasing shear rates ($n = 3, \bar{x} \pm s$)

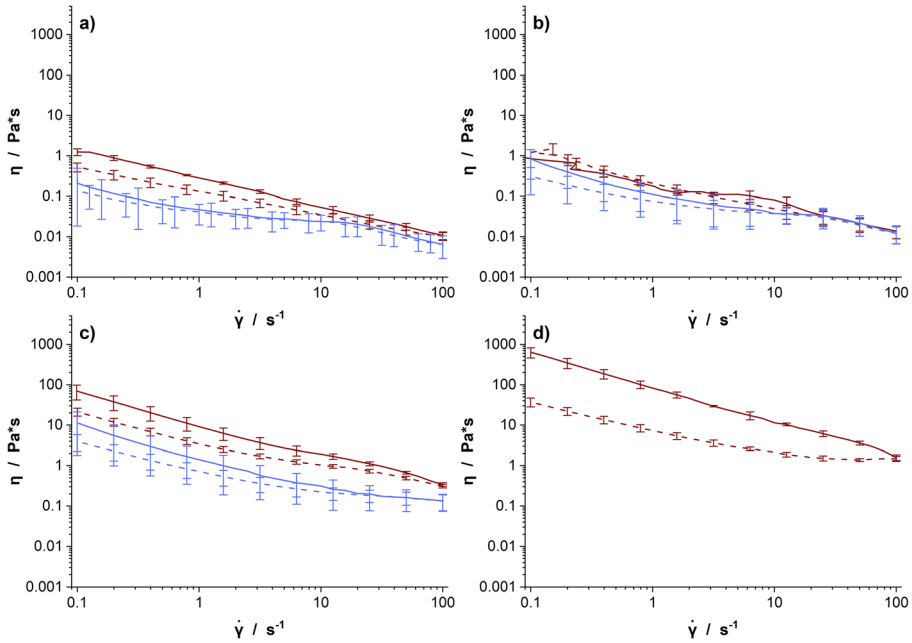

Fig. 3. Rheological investigation of MCC suspensions with (−) and without SLS (−) addition. **a** M1 and M5, **b** M2 and M6, **c** M3 and M7, and **d** M4. Solid lines represent increasing shear rates and dashed lines decreasing shear rates ($n = 3, \overline{x} \pm s$)

diffraction is limited when particle collectives with a broad distribution are examined due to the possibility of spectral overlapping. Also, other particle analyses like dynamic light scattering/photon correlation spectroscopy are limited in the analysis of broad PSDs. So, the real particle size could be much smaller than the one detected by these techniques. Another explanation might be found in the high surface area of MFC and NFC and the tendency to agglomerate during particle size analysis (38). Nevertheless, it was not intended to isolate pure MFC/NFC, but to investigate the impact of homogenization on the whole particle collective.

Homogenization of PC did not affect the fiber size of the sample in the same range as for MCC. For example, batch P6 (PC, 20 × 200 bar with SLS) resulted in a relative particle size reduction of 59% in x_{50}, whereas for MCC under the same conditions, a particle size reduction of 87% was observed for batch M6 (Table S3). As mentioned above, MCC is partially hydrolyzed and the elementary fibers are shorter than for PC. The average molecular weight of the used MCC was 41.0 ± 0.2 kDa and 152.3 ± 0.9 for PC. Kleinebudde et al. (39) found a correlation between the obtained particle size after homogenization and the DP of the used cellulose. Consequently, less energy was needed to loosen interfibrillar bonds and liberate NFC. MFC obtained from PC has a higher DP and therefore a higher aspect ratio because of the length of the micro fibrils (4). According to Moberg et al. (24), fibers with a higher aspect ratio, such as MFC from PC, should have a substantially lower percolation threshold than fibers with a low aspect ratio. This would also explain why PC suspensions showed higher viscosity then MCC suspensions even if the overall particle size was larger. The longer PC fibers are able to form a coherent matrix at lower volume fractions, and due to the higher length, these suspensions showed also a higher viscosity.

Statistical analysis of the x_{50}-value of PC suspensions did not show any significant factors (Fig. 4a). A non-significant tendency to smaller particles with increasing pressure was observed. An increase in pressure from 200 to 1200 bar led to an average particle size reduction of 10.3 μm. In case of MCC, the parameter number of cycles led to larger particles and also higher pressure showed a tendency to larger particles (Fig. 4b). This result was surprising but explainable.

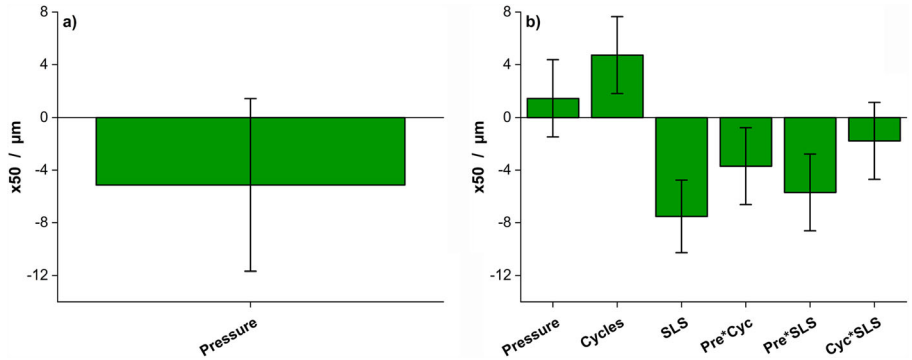

Fig. 4. Coefficient plot of effects on × 50 value for **a** PC and **b** MCC

By comparing the particle size of untreated MCC powder with the particle sizes of the homogenized forms, it becomes clear that particle size was strongly decreased by high pressure homogenization (Table S3). Yet, in the used factor space, higher pressures and more passes apparently led to larger particle sizes due to a tendency to re-agglomerate. This would also explain the strong negative impact of SLS on the measured particle size. SLS enhanced the electrostatic repulsion of the cellulose fibers. Cellulose flocculated to loosen agglomerates (40), which can be easily dispersed during laser diffraction analysis. The interactions *Pre*Cyc* suggests, that at low number of cycles, the effect of applied pressure was stronger, than in the case of higher number of cycles. *Pre*SLS* implies, that by adding SLS to the mixture, applied pressure now had a negative impact on particle size (Fig. S1). This result confirms that uncharged NFC tends to flocculate without surface modifications or surfactant addition (4,41).

Effect of Homogenization on the Casted Film Properties

Besides the suspension formation, homogenized cellulose also offers the possibility to form mechanically stable films (42). This characteristic was also attributed to the presence of colloidal fibers after homogenization. The mechanical stability of these films should be related to the PSD, the fraction of colloidal fibers and their morphology. For this reason, all produced suspensions were casted with a wet film thickness of 1000 μm. Not all suspensions resulted in uniform films after drying. With the exception of P6 (4 × 1200 bar + SLS), suspensions containing PC/SLS combinations did not form uniform films, the films had many defects or retained as powder on the liner. Suspensions without SLS formed uniform films, with the exception of P1, which also remained as loose powder on the liner. SEM images of the films reveal the change in particle morphology during homogenization (Figs. 5 and 6). In case of P1 (4 × 200 bar) (Fig. 5a), single fibers can still be identified. The degree of fibrillation was quite low and explains the missing film-forming property. However, with 20 cycles at 200 bar (Fig. 5b), PC formed a fiber network and a homogenous film could be obtained. P2 (4 × 1200 bar) (Fig. 5c) had a similar appearance to P3. Since the particle sizes of P2 (4 × 1200 bar) and P3 (20 × 200 bar) were quite similar (Table S3), this result is comprehensible. Process parameters of P4 (20 × 1200 bar) led to a less porous film with a fine fiber network (Fig. 5d). Due to the high viscosity of the suspension, it was not possible to distribute the suspension evenly on the aluminum foil liner. The result was a defective film that could not be used for further analysis of mechanical properties. Due to this, a statistical analysis using MLR was not possible for mechanical properties of the obtained films.

In case of MCC, even with M1, it was possible to obtain proper films without defects after drying. The surface structure (Fig. 6a) is smoother and less porous than the

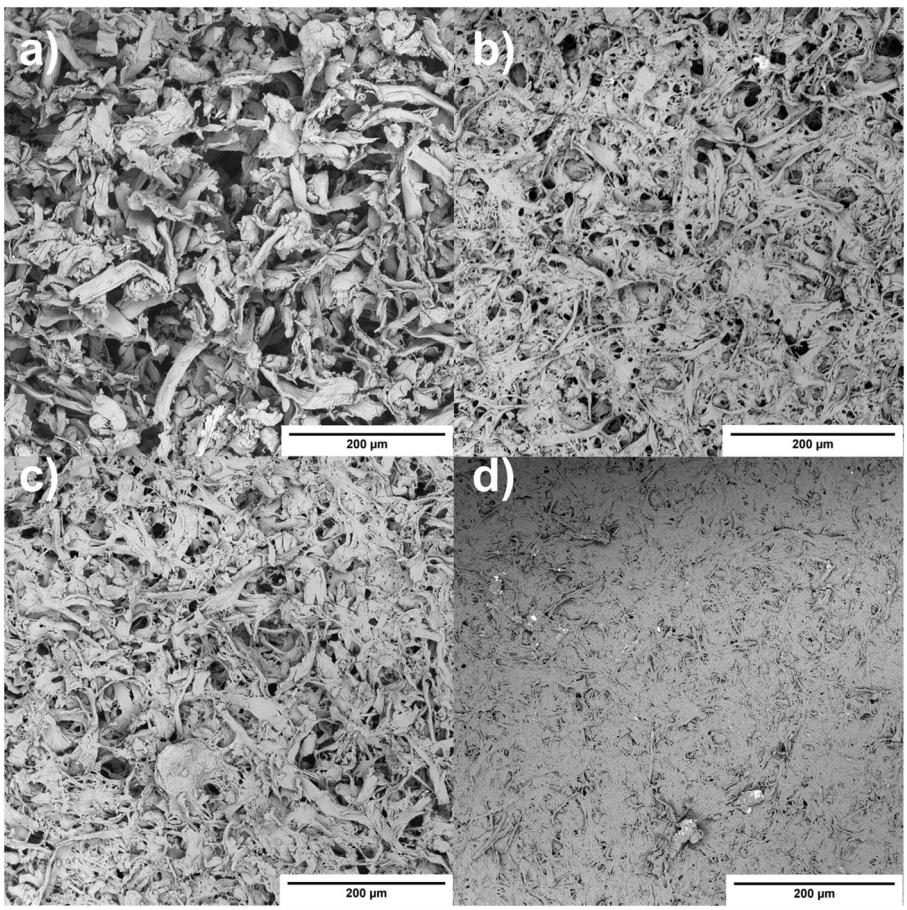

Fig. 5. SEM images of casted PC films dried at ambient conditions. **a** 4 × 200 bar (P1), **b** 20 × 200 bar (P3), **c** 4 × 1200 bar (P2), and **d** 20 × 1200 bar (P4)

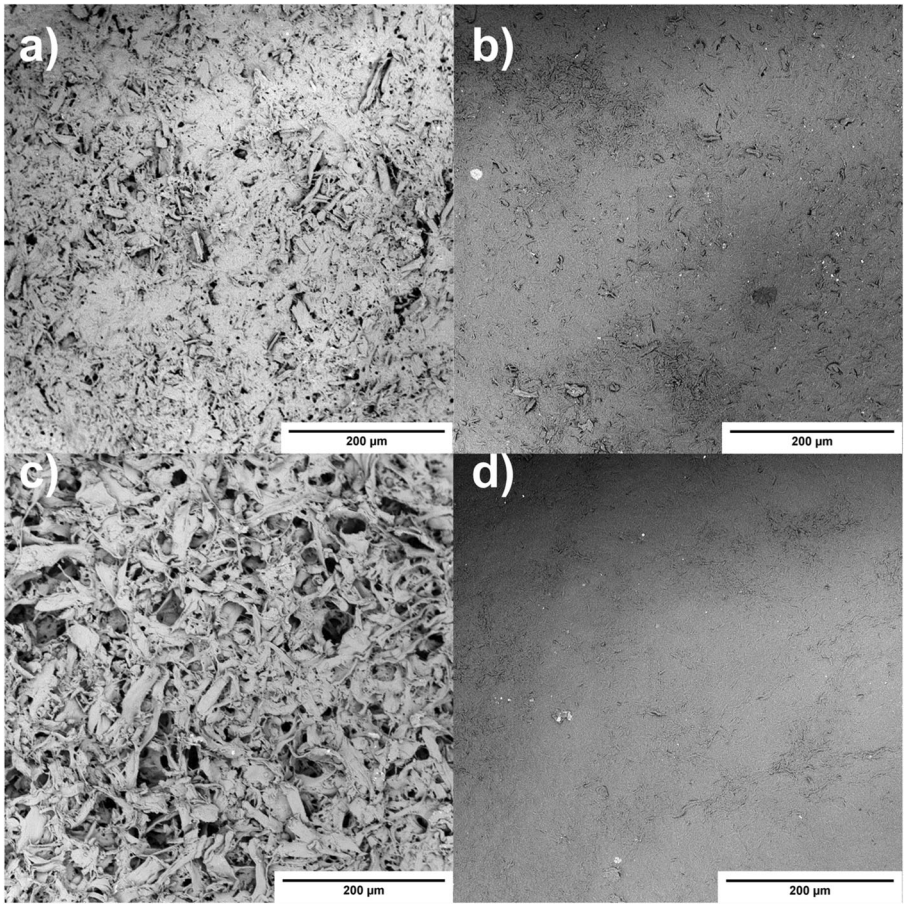

Fig. 6. SEM images of MCC suspensions dried under ambient conditions. **a** 4 × 200 bar (M1), **b** 20 × 200 bar (M3), **c** 4 × 1200 bar (M2), and **d** 20 × 1200 bar (M4)

equivalent experiment of PC (P1). With more homogenization cycles and higher pressures, surfaces became even smoother until no single unit could be identified anymore (Fig. 6b, d). In case of M2 (Fig. 6c), increased agglomeration might be responsible for the quite fibrous appearance. As with PC, the addition of SLS led to cracked and perforated films, which cannot be used for analysis. Overall, MCC led to a smoother surface structure than PC did. The smaller NFC fibers liberated from homogenized MCC have a larger specific surface and therefore higher interaction area. During drying, the capillary forces contracted the particles together closely and facilitated the formation of smooth surface structures with few pores. This behavior is well known for the drying of pellets containing MCC as pelletizing aid (43). Similarly, MCC pellets shrink and result in very smooth and dense surfaces. This behavior has been attributed to the autohesion phenomenon known from insoluble polymers (44). In the case of PC, the fibers were larger and the capillary forces in wet stage decreased (45,46). Consequently, the PC films were less densified and more porous under the same conditions.

The measured mechanical properties of the obtained cellulose sheets are displayed in Fig. 7 a and b. Cellulose sheets show relatively low E_t, σ_b and ε_B. The measured values were dramatically lower than results reported in literature. For sheets produced with MFC obtained from spruce pulp, a Young's modulus of 15.7 GPa and a tensile strength of about 104 MPa were reached (42). For Films containing NFC, similar mechanical properties are reported (47). A possible explanation for these discrepancies might be found in the broad PSD of the cellulose fibers (Table S3). The broad PSD resulted in defects in the film surface, due to the lower specific surface area of the larger fibers and therefore a weaker interaction in the whole fiber network. In case of MCC films, a correlation between the particle span and the resulting σ_b, respectively, E_t could be observed (Fig. 7d). A similar correlation could not be found for PC films (Fig. 7c). Another explanation might be found in the production method. In both studies, simple convective drying of the gel in a vessel was performed instead of using a film coating bench. The casting method might also resulted in more structural defects due to possible inhomogenities on the liner. It should be noted that the solvent casting method is normally used for soluble polymers and not for insoluble film formers (48).

Nevertheless, MCC suspensions formed more stable films than PC. Considering the SEM pictures of the films, it becomes clear that the difference in mechanical properties can be attributed to the lower porosity of MCC films. This is again a consequence of the partial hydrolysis and the generally lower interfibrillar bonding forces of cellulose chains. Under the same conditions, it was possible to obtain more fine fibers with high specific surface area and the capability to form intrafibrillar hydrogen bonds which were mainly responsible for the mechanical stability of MCC films

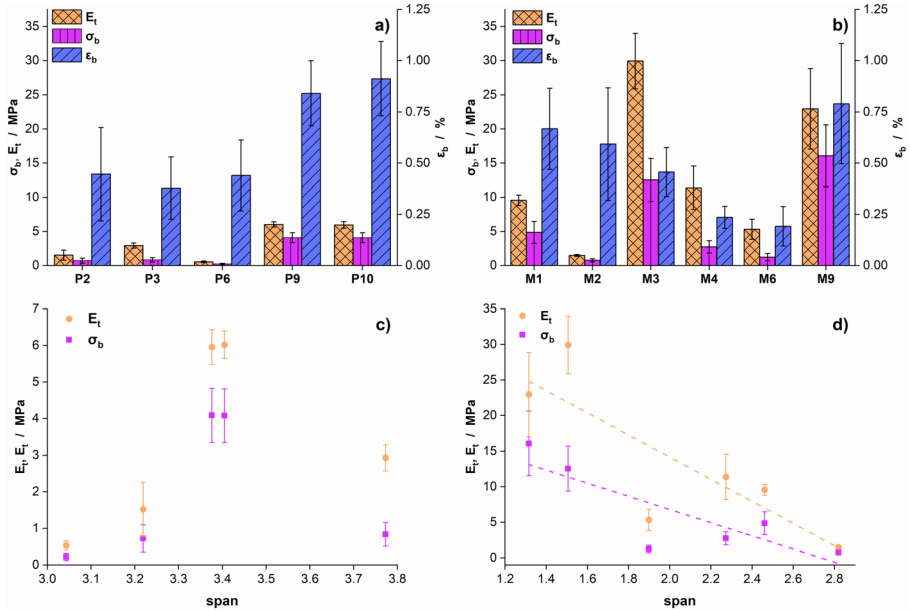

Fig. 7. Upper row: mechanical properties of obtained films from statistical experiments from **a** PC and **b** MCC ($n > 4$, $\bar{x} \pm$ CI, $\alpha = 0.05$). Bottom row: correlation of span and resulting mechanical properties for **c** PC films and **d** MCC films (E_t: R: −0.827, σ_b: R: −0.834) ($n > 4$, $\bar{x} \pm$ CI, $\alpha = 0.05$)

(4). The longer fibers obtained from PC formed a more paper-like network structure with larger pores and a lower contact area of the fibers and therefore worse mechanical properties.

By comparing M1 and M3, the effect of the number of cycles can be estimated (Fig. 7b). With an increase in the number of cycles from 4 to 20 with an equal pressure drop of 200 bar, the films obtained higher mechanical stability and stiffness. At higher pressures of 1200 bar, *e.g.*, M2 and M4 (Fig. 7b), the effect was not as strong as for batches M1/M3. The viscosity of M4 was approximately ten times higher than M3 (Table S3). This high viscosity resulted in difficulties during film casting and more structural defects of the films. These structural defects are the main cause for the worse mechanical properties. These effects could not be proven for PC films, due to production difficulties. Nevertheless, P1 did not form any stable film, whereas it was possible to produce cellulose films using P3 (Fig. 7a). This indicates that the number of cycles is more critical during homogenization. These results can also be confirmed with results from viscosity measurements, where the the number of cycles had a significant effect on the resulting suspension viscosity. Stelte and Sanadi (49) have reported similar results regarding the effect of number of cycles on resulting mechanical properties and correlated this with a higher fraction of NFC at higher amount of homogenization cycles. PC suspensions produced at the center point (P9 and P10) formed the most stable films after drying. These process parameters seemed to be an optimum for PC and were quite similar to common process parameters reported in literature (27).

High-pressure homogenization of both, PC and MCC suspensions, led to film formation properties, but with some substantial differences. While homogenization of MCC suspensions was feasible without clogging of the valves, clogging during homogenization of PC suspensions occurred frequently. All differences can probably be attributed to the different particle size and fiber morphologies. The longer MFC fibers resulted in higher viscosity than the shorter NFC. This behavior is well known from soluble polymers, where the DP/average molecular weight is a key parameter for the resulting viscosity. However, the larger size and the lower amount of MFC in PC suspensions led to a higher sensitivity to SLS and films with worse mechanical properties.

Pharmaceutical Application of MFC/NFC

The film-forming properties of homogenized cellulose opens up new fields of application, *e.g.*, as film former for the production of orodispersible films (ODF). In this part, the application for MFC/NFC suspensions as carrier platform for orodispersible films was investigated. Based on the results from the homogenization study, MCC and PC were homogenized at 750 bar for 10 cycles with a solid cotent of 5% (m/m), to obtain suspensions with adequate rheological properties in dispersed stage and suitable mechanical properties as film. For ODFs, a fast disintigration to easily swallowable particles is an important criterion (48) for the use in special patient groups, like children or elderly people. In addition, suitable mechanical properties are needed to ensure easy application without premature fractures. For this reason, different mixtures of homogenized PC and MCC suspensions were used for the production of the sheets. Incorporation of an additional plasticizer was not necessary to obtain films with suitable flexibility.

The mechanical stability of the casted cellulose sheets could be correlated with the fraction of PC used in the suspension (Fig. 8). With decreasing PC fraction, σ_b and E_t increased, whereas ε_b was not be affected significantly by PC fraction. The results for pure PC films, respectively, MCC films were consistent with the results of the films from the previous experiments (Fig. 7a, b). Although the films gained mechanical stability, rapid disintegration is also a necessary

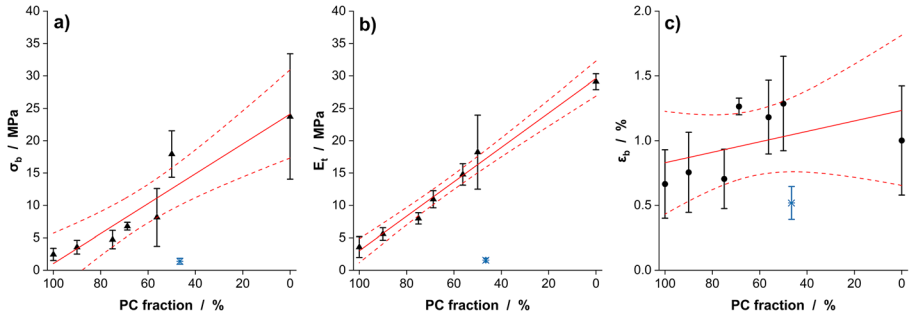

Fig. 8. Mechanical properties of cellulose sheets with varying fraction of PC (σ_b: R: −0.9388; E_t: R: −0.9921; ε_b: R: −0.4889). **x** indicating results for API-loaded PC films ($n > 4$; $\bar{x} \pm$ CI, $\alpha = 0.05$)

requirement for the use as ODF. Only films containing pure PC or 10% (m/m) of MCC showed disintegration within 30 s and fullfiled the requirements for orodispersible dosage forms according to USP (Table 3). The average film thicknesses varied with PC fraction. With decreasing PC fraction in the suspensions, films became thinner. At a PC fraction below 75% (m/m), a reduced film thickness in a similar range as films containing pure MCC was obtained.

DCS is a nonsteroidal anti-inflammatory drug with a maximum daily dosage of 150 mg for an adult. The target dose was set to 25 mg per sheet with the dimensions of 2 cm × 3 cm (6 cm^2). This is a common dosage in the treatment of moderate pain. To investigate the feasibility of drug loading in orodispersible PC sheets, DCS was mixed with homogenized PC suspension and casted. Sheets with MCC as film-forming polymer were not investigated due to the lack in disintegration of these films. Kolakovic et al. (21) reported extended release profile for films made of NFC and, hence, this usage of MCC did not appear plausible for the manufactering of ODFs.

Incorporation of DCS into PC films resulted in thicker films after drying (Table 3). This was a result of the increased solid content of the film suspensions (5% *vs.* 8%) and the particle size of DCS. The API particles were incorporated into the cellulose fiber matrix and also sticking on the surface of the films (Fig. 9). Mechanical stability was decreased by added DCS and even lower than for sheets out of pure PC (Fig. 8). API crystals may interfere with the cellulose matrix and led to weaker bonding forces between the fibers. Removal of the dried films and handling was difficult due to brittle nature of the films. The average sheet weight was 52.9 ± 1.28 mg resulting in a drug load of approximately 47%. This high drug load might be the main reason for the poor mechanical properties. Nevertheless, the content uniformity investigation (Table S4) resulted in an acceptance value of 5.84 and therefore fullfil the requirements of European Pharmacopeia.

Since the drug load for conventional ODFs is limited to highly potent APIs (48), PC films open the opportunity to produce films with a drug load of about 50% by weight. Although the high drug load resulted in relatively poor mechanical stability of DCS films, the mechanical properties were still acceptable. In addition, homogenized PC suspensions might be useful for drugs with lower dosages. This would not affect the mechanical properties in the same manner and improve the handling of the ODFs.

A possible application for PC films might be the usage as basis for pharmaceutical 2D printing processes (50,51). The porous structure of the resulting films and the high swelling capability of cellulose might facilitate an easy absorption of the printing fluid and enabling higher drug loads without affecting the meachnical properties. But more research is needed to evaluate possible application areas for homogenized PC as film-forming polymer.

Table 3. Disintegration times and film thicknesses of produced films (thickness: $n = 10$, $\bar{x} \pm$ CI, $\alpha = 0.05$)

PC content [m/m]/%	Disintegration time/s	Thickness/μm
100	13	120.2 ± 14.9
90	30	126.3 ± 12.9
75	> 180	112.2 ± 5.4
68.75	> 180	83.1 ± 10.2
56.25	> 180	75.5 ± 6.0
50	> 180	61.7 ± 6.7
0	> 180	63.9 ± 8.0
DCS loaded	12	258.9 ± 1.0

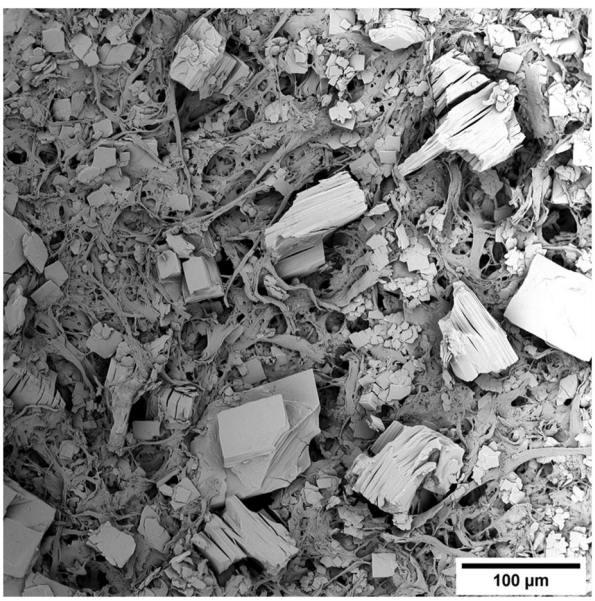

Fig. 9. SEM picture of a DCS-loaded film

CONCLUSIONS

Particle size of PC and MCC was sucessfully reduced by high-pressure homogenization. Furthermore, critical process parameters of the homogenization process were identified. Homogenization of MCC led to suspensions with smaller particles due to lower DP and lower intrafibrillar bonding forces as a result of the previous hydrolysis step. The lower viscosity was a result of the NFC morphology. In contrast to MFC, NFC is shorter with lower aspect ratio and resulting analogous to soluble polymers in a lower viscosity. The addition of SLS reduced the viscosity of the cellulose suspensions due to increased electrostatic repulsion of the colloidal MFC/NFC and resulted in cellulose matrix defects but also to a faster matrix regeneration. PC as more fibrous and coarse grade is more affected by SLS probably due to the lower specific surface area.

After homogenization, both cellulose grades show film-forming properties. MCC resulted in films with higher mechanical stability than PC. These differences are considerably smaller after further homogenization. Particle size and fiber morphology have an impact on the resulting film characteristics. MCC forms dense films with low porosity due to the small particle size and the lower aspect ratio of the obtained NFC, whereas PC forms more paper-like films with high porosity. These results might be transferable to other processes, like wet-extrusion/spheronization and would support the finding of our previous study (20), where homogenized PC was sucessfully used as pelletizing agent.

Drug loading of films containing homogenized PC as film former facilitated a high drug load of about 50% and rapid disintegration in less than 30 s. The mechanical stability was affected by the high drug load. However, considering the high drug content, the mechanical properties were still acceptable. It is also advantageous that no additional plasticizer was required to ensure suffcient flexibility of the ODFs. Due to the porous structure of the PC films, other applications, for example as printing basis for pharmaceutical 2D printing processes, are possible.

ACKNOWLEDGMENTS

The authors would like to thank JRS Pharma GmbH for supplying the powdered cellulose and microcrystalline cellulose used in this study. The authors would also like to thank Anna-Lena Beiersmann and Julia Stock for the execution of several experiments.

COMPLIANCE WITH ETHICAL STANDARDS

Conflict of Interest The authors declare that they have no conflict of interest.

REFERENCES

1. Kamel S, Ali N, Jahangir K, Shah SM, El-Gendy AA. Pharmaceutical significance of cellulose: a review. Express Polym Lett. 2008;2(11):758–78.
2. Klemm D, Heublein B, Fink HP, Bohn A. Cellulose: fascinating biopolymer and sustainable raw material. Angew Chem Int Ed Engl. 2005;44(22):3358–93.
3. Qua EH, Hornsby PR, Sharma HSS, Lyons G. Preparation and characterisation of cellulose nanofibres. J Mater Sci. 2011;46(18):6029–45.
4. Klemm D, Kramer F, Moritz S, Lindstrom T, Ankerfors M, Gray D, et al. Nanocelluloses: a new family of nature-based materials. Angew Chem Int Ed Engl. 2011;50(24):5438–66.
5. Battista OA. Hydrolysis and crystallization of cellulose. Ind Eng Chem. 1950;42(3):502–7.
6. Battista OA, Smith PA. Microcrystalline Cellulose - Oldest Polymer Finds New Industrial Uses. Ind Eng Chem. 1962;54(9):20.
7. Reynolds AD. A New Technique for Production of Spherical Particles. Manuf Chemist. 1970;41(6):40.
8. Newton JM. Extrusion and extruders. In: Swarbrick J, editor. Encyclopedia of pharmaceutical technology. 3. 3rd ed. Boca Raton: Taylor & Francis; 2007. p. 1712–28.
9. Fielden KE, Newton JM, O'Brien P, Rowe RC. Thermal studies on the interaction of water and microcrystalline cellulose. J Pharm Pharmacol. 1988;40(10):674–8.
10. Ek R, Newton JM. Microcrystalline cellulose as a sponge as an alternative concept to the crystallite-gel model for extrusion and spheronization. Pharm Res. 1998;15(4):509–12.
11. Tomer G, Newton JM. Water movement evaluation during extrusion of wet powder masses by collecting extrudate fractions. Int J Pharm. 1999;182(1):71–7.
12. Rough SL, Bridgwater J, Wilson DI. Effects of liquid phase migration on extrusion of microcrystalline cellulose pastes. Int J Pharm. 2000;204(1–2):117–26.
13. Luukkonen P, Newton JM, Podczeck F, Yliruusi J. Use of a capillary rheometer to evaluate the rheological properties of microcrystalline cellulose and silicified microcrystalline cellulose wet masses. Int J Pharm. 2001;216(1–2):147–57.
14. Luukkonen P, Maloney T, Rantanen J, Paulapuro H, Yliruusi J. Microcrystalline cellulose-water interaction–a novel approach using thermoporosimetry. Pharm Res. 2001;18(11):1562–9.
15. Fechner PM, Wartewig S, Futing M, Heilmann A, Neubert RH, Kleinebudde P. Properties of microcrystalline cellulose and powder cellulose after extrusion/spheronization as studied by fourier transform Raman spectroscopy and environmental scanning electron microscopy. AAPS PharmSci. 2003;5(4):E31.
16. Kleinebudde P. The crystallite-gel-model for microcrystalline cellulose in wet-granulation, extrusion, and spheronization. Pharm Res. 1997;14(6):804–9.
17. Suzuki T, Kikuchi H, Yamamura S, Terada K, Yamamoto K. The change in characteristics of microcrystalline cellulose during wet granulation using a high-shear mixer. J Pharm Pharmacol. 2001;53(5):609–16.
18. Sarkar S, Heng PW, Liew CV. Insights into the functionality of pelletization aid in pelletization by extrusion-spheronization. Pharm Dev Technol. 2013;18(1):61–72.
19. Sarkar S, Liew CV. Moistening liquid-dependent de-aggregation of microcrystalline cellulose and its impact on pellet formation by extrusion-spheronization. AAPS PharmSciTech. 2014;15(3):753–61.
20. Lenhart V, Quodbach J, Kleinebudde P. Mechanistic understanding regarding the functionality of microcrystalline cellulose and powdered cellulose as pelletization aids in wet-extrusion/spheronization. Cellulose. 2019. https://doi.org/10.1007/s10570-019-02895-y
21. Kolakovic R, Peltonen L, Laukkanen A, Hirvonen J, Laaksonen T. Nanofibrillar cellulose films for controlled drug delivery. Eur J Pharm Biopharm. 2012;82(2):308–15.
22. Kolakovic R, Peltonen L, Laaksonen T, Putkisto K, Laukkanen A, Hirvonen J. Spray-dried cellulose nanofibers as novel tablet excipient. AAPS PharmSciTech. 2011;12(4):1366–73.
23. Xu X, Liu F, Jiang L, Zhu JY, Haagenson D, Wiesenborn DP. Cellulose nanocrystals vs. cellulose nanofibrils: a comparative study on their microstructures and effects as polymer reinforcing agents. ACS Appl Mater Interfaces. 2013;5(8):2999–3009.
24. Moberg T, Sahlin K, Yao K, Geng SY, Westman G, Zhou Q, et al. Rheological properties of nanocellulose suspensions: effects of fibril/particle dimensions and surface characteristics. Cellulose. 2017;24(6):2499–510.
25. DIN EN ISO 527-1:2012, Plastics - Determination of tensile properties - Part 1: General principles (ISO 527-1:2012). 2012.

26. Preis M, Woertz C, Kleinebudde P, Breitkreutz J. Oromucosal film preparations: classification and characterization methods. Expert Opin Drug Deliv. 2013;10(9):1303–17.
27. Jonoobi M, Oladi R, Davoudpour Y, Oksman K, Dufresne A, Hamzeh Y, et al. Different preparation methods and properties of nanostructured cellulose from various natural resources and residues: a review. Cellulose. 2015;22(2):935–69.
28. Turbak AF, Snyder FW, Sandberg KR, editors. Microfibrillated cellulose, a new cellulose product: properties, uses, and commercial potential. J Appl Polym Sci Appl Polym Symp;(United States). Shelton: ITT Rayonier Inc.; 1983.
29. Taheri H, Samyn P. Effect of homogenization (microfluidization) process parameters in mechanical production of micro- and nanofibrillated cellulose on its rheological and morphological properties. Cellulose. 2016;23(2):1221–38.
30. Floury J, Desrumaux A, Lardières J. Effect of high-pressure homogenization on droplet size distributions and rheological properties of model oil-in-water emulsions. Innovative Food Sci Emerg Technol. 2000;1(2):127–34.
31. Qian C, McClements DJ. Formation of nanoemulsions stabilized by model food-grade emulsifiers using high-pressure homogenization: factors affecting particle size. Food Hydrocoll. 2011;25(5):1000–8.
32. Lee SY, Chun SJ, Kang IA, Park JY. Preparation of cellulose nanofibrils by high-pressure homogenizer and cellulose-based composite films. J Ind Eng Chem. 2009;15(1):50–5.
33. Lamprecht A, Ubrich N, Hombreiro Perez M, Lehr C, Hoffman M, Maincent P. Influences of process parameters on nanoparticle preparation performed by a double emulsion pressure homogenization technique. Int J Pharm. 2000;196(2):177–82.
34. Paakko M, Ankerfors M, Kosonen H, Nykanen A, Ahola S, Osterberg M, et al. Enzymatic hydrolysis combined with mechanical shearing and high-pressure homogenization for nanoscale cellulose fibrils and strong gels. Biomacromolecules. 2007;8(6):1934–41.
35. Li J, Wei X, Wang Q, Chen J, Chang G, Kong L, et al. Homogeneous isolation of nanocellulose from sugarcane bagasse by high pressure homogenization. Carbohydr Polym. 2012;90(4):1609–13.
36. Quennouz N, Hashmi SM, Choi HS, Kim JW, Osuji CO. Rheology of cellulose nanofibrils in the presence of surfactants. Soft Matter. 2016;12(1):157–64.
37. Iotti M, Gregersen OW, Moe S, Lenes M. Rheological studies of Microfibrillar cellulose water dispersions. J Polym Environ. 2011;19(1):137–45.
38. Saarikoski E, Saarinen T, Salmela J, Seppala J. Flocculated flow of microfibrillated cellulose water suspensions: an imaging approach for characterisation of rheological behaviour. Cellulose. 2012;19(3):647–59.
39. Kleinebudde P, Jumaa M, El Saleh F. Influence of the degree of polymerization on the behavior of cellulose during homogenization and extrusion/spheronization. AAPS PharmSci. 2000;2(3):E21.
40. Hu Z, Cranston ED, Ng R, Pelton R. Tuning cellulose nanocrystal gelation with polysaccharides and surfactants. Langmuir. 2014;30(10):2684–92.
41. Fall AB, Lindstrom SB, Sundman O, Odberg L, Wagberg L. Colloidal stability of aqueous nanofibrillated cellulose dispersions. Langmuir. 2011;27(18):11332–8.
42. Syverud K, Stenius P. Strength and barrier properties of MFC films. Cellulose. 2008;16(1):75–85.
43. Kleinebudde P. Shrinking and swelling properties of pellets containing microcrystalline cellulose and low substituted hydroxypropylcellulose: II Swelling properties. Int J Pharm. 1994;109(3):221–7.
44. Millili GP, Wigent RJ, Schwartz JB. Autohesion in pharmaceutical solids. Drug Dev Ind Pharm. 1990;16(16):2383–407.
45. Pietsch W, Hoffman E, Rumpf H. Tensile Strength of Moist Agglomerates. End Eng Chem Prod Res Dev. 1969;8(1):58.
46. Pietsch W, Rumpf H. Haftkraft, Kapillardruck, Flüssigkeitsvolumen und Grenzwinkel einer Flüssigkeitsbrücke zwischen zwei Kugeln. Chem-Ing-Tech. 1967;39(15):885–93.
47. Benitez AJ, Torres-Rendon J, Poutanen M, Walther A. Humidity and multiscale structure govern mechanical properties and deformation modes in films of native cellulose nanofibrils. Biomacromolecules. 2013;14(12):4497–506.
48. Hoffmann EM, Breitenbach A, Breitkreutz J. Advances in orodispersible films for drug delivery. Expert Opin Drug Deliv. 2011;8(3):299–316.
49. Stelte W, Sanadi AR. Preparation and characterization of cellulose nanofibers from two commercial hardwood and softwood pulps. Ind Eng Chem Res. 2009;48(24):11211–9.
50. Daly R, Harrington TS, Martin GD, Hutchings IM. Inkjet printing for pharmaceutics - a review of research and manufacturing. Int J Pharm. 2015;494(2):554–67.
51. Thabet Y, Sibanc R, Breitkreutz J. Printing pharmaceuticals by inkjet technology: proof of concept for stand-alone and continuous in-line printing on orodispersible films. J Manuf Process. 2018;35:205–15.